

2020

Evolutionary Determinism and Convergence Associated with Water Column Transitions in Marine Fishes

Melissa Rincon-Sandoval

Emmanuelle Duarte-Ribeiro

Aaron M. Davis

Aintzane Santaquiteria

Lily C. Hughes

See next page for additional authors

Follow this and additional works at: https://digitalcommons.odu.edu/biology_fac_pubs



Part of the [Aquaculture and Fisheries Commons](#), [Biology Commons](#), and the [Ecology and Evolutionary Biology Commons](#)

Original Publication Citation

Rincon-Sandoval, M., Duarte-Ribeiro, E., Davis, A. M., Santaquiteria, A., Hughes, L. C., Baldwin, C. C., Soto-Torres, L., Acero, P. A., Walker, H. J., Jr., Carpenter, K. E., Sheaves, M., Ortí, G., Arcila, D., & Betancur, R. R. (2020). Evolutionary determinism and convergence associated with water-column transitions in marine fishes. *Proceedings of the National Academy of Sciences of the United States of America*, 117(52), 33396-33403. <https://doi.org/10.1073/pnas.2006511117>

This Article is brought to you for free and open access by the Biological Sciences at ODU Digital Commons. It has been accepted for inclusion in Biological Sciences Faculty Publications by an authorized administrator of ODU Digital Commons. For more information, please contact digitalcommons@odu.edu.

Authors

Melissa Rincon-Sandoval, Emmanuelle Duarte-Ribeiro, Aaron M. Davis, Aintzane Santaquiteria, Lily C. Hughes, Carole C. Baldwin, Luisángely Soto-Torres, Arturo Acero P., H.J. Walker Jr, Kent E. Carpenter, Marcus Sheaves, Guillermo Orti, Dahiana Arcila, and Ricardo Betancur-R.



Evolutionary determinism and convergence associated with water-column transitions in marine fishes

Melissa Rincon-Sandoval^{a,b,1}, Emanuell Duarte-Ribeiro^{a,1,2}, Aaron M. Davis^c, Aintzane Santaquiteria^a, Lily C. Hughes^{d,e}, Carole C. Baldwin^e, Luisángely Soto-Torres^f, Arturo Acero P.^b, H. J. Walker Jr^g, Kent E. Carpenter^h, Marcus Sheavesⁱ, Guillermo Orti^{d,e}, Dahiana Arcila^{a,j}, and Ricardo Betancur-R.^{a,1,2}

^aDepartment of Biology, The University of Oklahoma, Norman, OK 73019; ^bUniversidad Nacional de Colombia sede Caribe, Centro de Estudios en Ciencias del Mar (CECIMAR), Santa Marta, Magdalena, Colombia; ^cCentre for Tropical Water and Aquatic Ecosystem Research, School of Marine and Tropical Biology, James Cook University, Townsville, QLD 4811, Australia; ^dDepartment of Biological Sciences, The George Washington University, Washington, DC 20052; ^eDepartment of Vertebrate Zoology, National Museum of Natural History, Smithsonian Institution, Washington, DC 20560; ^fDepartment of Biology, Universidad de Puerto Rico—Río Piedras, San Juan Puerto Rico, 00931; ^gScripps Institution of Oceanography, University of California San Diego, La Jolla, CA 92093-0244; ^hBiological Sciences, Old Dominion University, Norfolk, VA 23529; ⁱMarine Data Technology Hub, James Cook University, Townsville, QLD 4811, Australia; and ^jDepartment of Ichthyology, Sam Noble Oklahoma Museum of Natural History, Norman, OK

Edited by David M. Hillis, The University of Texas at Austin, Austin, TX, and approved November 12, 2020 (received for review April 6, 2020)

Repeatable, convergent outcomes are *prima facie* evidence for determinism in evolutionary processes. Among fishes, well-known examples include microevolutionary habitat transitions into the water column, where freshwater populations (e.g., sticklebacks, cichlids, and whitefishes) recurrently diverge toward slender-bodied pelagic forms and deep-bodied benthic forms. However, the consequences of such processes at deeper macroevolutionary scales in the marine environment are less clear. We applied a phylogenomics-based integrative, comparative approach to test hypotheses about the scope and strength of convergence in a marine fish clade with a worldwide distribution (snappers and fusiliers, family Lutjanidae) featuring multiple water-column transitions over the past 45 million years. We collected genome-wide exon data for 110 (~80%) species in the group and aggregated data layers for body shape, habitat occupancy, geographic distribution, and paleontological and geological information. We also implemented approaches using genomic subsets to account for phylogenetic uncertainty in comparative analyses. Our results show independent incursions into the water column by ancestral benthic lineages in all major oceanic basins. These evolutionary transitions are persistently associated with convergent phenotypes, where deep-bodied benthic forms with truncate caudal fins repeatedly evolve into slender midwater species with furcate caudal fins. Lineage diversification and transition dynamics vary asymmetrically between habitats, with benthic lineages diversifying faster and colonizing midwater habitats more often than the reverse. Convergent ecological and functional phenotypes along the benthic–pelagic axis are pervasive among different lineages and across vastly different evolutionary scales, achieving predictable high-fitness solutions for similar environmental challenges, ultimately demonstrating strong determinism in fish body-shape evolution.

phylogenomics | macroevolution | habitat transitions | benthic–pelagic axis | Lutjanidae

A question of central interest in biology is whether evolutionary outcomes can be predictable and thoroughly governed by the laws of nature or contingent on a sequence of unpredictable historical events, such as rare environmental catastrophes, which may be sensitive to circumstances inherent to particular evolutionary paths (1, 2). Reconciling this conundrum may depend largely upon the scope and strength of evolutionary convergence—the process whereby natural selection tends to produce a limited set of high-fitness solutions when confronted with similar challenges imposed by the environment (i.e., the adaptive landscape). Convergence ranks among the most conspicuous features in biodiversity, and the general mechanisms by which the physical constants of nature constrain morphological outcomes have been recognized for decades (3–5). Nevertheless,

the deterministic nature of the processes leading to convergent evolution is still contentious (6, 7).

An emblematic example of evolutionary convergence comes from aquatic environments, where distantly related pelagic lineages tend to evolve similar body plans. Based on these observations, G. McGhee hypothesized that there are limited ways to build a fast-swimming aquatic organism, which is why dolphins, swordfish, sharks, and ichthyosaurs all present streamlined fusiform bodies—a nontrivial adaptation to the locomotion constraints imposed by the viscosity of water and drag flow (8). In ray-finned fishes (Actinopterygii), the evolution of fusiform body plans also has a strong adaptive basis and is frequently associated with the invasion of the water column by primarily benthic lineages. Body elongation has been recognized as the primary axis of diversification in fishes (9–13), and evidence supporting this deterministic process comes from a broad spatiotemporal spectrum. At a narrow scale, post-Pleistocene parallel invasions of freshwater lakes by marine three-spined

Significance

Body shape is a strong predictor of habitat occupation in fishes, which changes rapidly at microevolutionary scales in well-studied freshwater systems such as sticklebacks and cichlids. Deep-bodied forms tend to occur in benthic habitats, while pelagic species typically have streamlined body plans. The recurrent evolution of this pattern across distantly related groups suggests that limited sets of high-fitness solutions exist due to environmental constraints. We rigorously test these observations showing that similar constraints operate at deeper evolutionary scales in a clade (Lutjanidae) of primarily benthic fish dwellers that repeatedly transitioned into midwater habitats in all major oceans throughout its 45-million-year history. Midwater species strongly converge in body shape, emphasizing evolutionary determinism in form and function along the benthic–pelagic axis.

Author contributions: M.R.-S., E.D.-R., A.M.D., and R.B.-R. designed research; C.C.B., A.A.P., H.J.W., K.E.C., M.S., G.O., and D.A. curated and contributed specimens; M.R.-S., E.D.-R., A.S., L.C.H., L.S.-T., G.O., D.A., and R.B.-R. analyzed data and performed research; and M.R.-S., E.D.-R., G.O., and R.B.-R. wrote the paper.

The authors declare no competing interest.

This article is a PNAS Direct Submission.

Published under the PNAS license.

¹M.R.-S., E.D.-R., and R.B.-R. contributed equally to the work.

²To whom correspondence may be addressed. Email: ricardo.betancur@ou.edu or emanuell.ribeiro@ou.edu.

This article contains supporting information online at <https://www.pnas.org/lookup/suppl/doi:10.1073/pnas.200651117/-DCSupplemental>.

First published December 16, 2020.

stickleback populations have repeatedly triggered the evolution of two divergent phenotypes, a deep-body form associated with more benthic habitats and a slender-body form that occurs in the water column (14, 15). Quantitative assessments at microevolutionary scales have documented similar cases of resource partitioning on sympatric populations of cichlids and European whitefishes, among others (11, 16–19). At the other end of the evolutionary spectrum, evidence from the fossil record shows a significant component of the Paleogene spiny-rayed teleost (acanthomorph) radiation that colonized areas of the morphospace previously occupied by incumbent pelagic species that became extinct during the Cretaceous–Paleogene (K–Pg) mass extinction (12, 20).

Here, we assess the role of convergent evolution associated with transitions along the benthic–pelagic axis in a clade of tropical and subtropical marine fishes—the snappers and fusiliers in the family Lutjanidae—that bridge both ends of the evolutionary continuum. Previous studies have shown that lutjanids include a number of independent lineages that have undergone niche partitioning along the water column and that this ecological divergence is seemingly associated with different configurations in feeding ecology and body elongation (21–23). Based on these observations, we first test the hypothesis that independent incursions into the water column in this group are constrained to a narrow portion of the adaptive landscape. Second, given the widespread distribution of this family and the potential temporal range of habitat transitions in the clade, we hypothesize that these evolutionary transitions have occurred independently within all major oceanic basins where the family is distributed, providing strong evidence that functional constraints in open water habitats shape phenotypic evolution in fishes in particular and aquatic vertebrates more generally.

Community ecology studies have demonstrated that marine biodiversity is higher in benthic than pelagic environments (24), suggesting that the adoption of the midwater lifestyle by lutjanids may have resulted in an “evolutionary ratchet,” where the acquisition of specialized traits are selectively advantageous in the short term but, in the long term, can create an evolutionary trap due to lowered speciation or elevated extinction rates (25). This hypothesis makes two predictions: 1) habitat transitions from benthic to midwater systems are expected to be unidirectional or asymmetric, and 2) the microhabitat homogeneity of pelagic systems provides fewer opportunities for diversification than benthic environments, where multiple niches may cooccur.

To address these questions using rigorous quantitative approaches, we estimated a set of taxonomically rich time trees for lutjanids based on genome-wide data and used an integrative comparative dataset that includes morphological and ecological data layers in combination with geographic distribution data. By conducting a suite of phylogenetic comparative analyses using independent genomic subsets, we examined the temporal and geographic scope of evolutionary convergence among midwater snapper and fusilier lineages. These analyses show that repeated habitat transitions from bottom to midwater systems are linked strongly to patterns of evolutionary convergence in body shape and also are associated with asymmetric habitat transitions and slower rates of lineage diversification. These transitions took place independently within all major oceanic basins. Taken together, our findings ultimately reinforce the deterministic nature of evolution as a consequence of the similar use of the niche space along the benthic–pelagic axis.

Results

Phylogenomic Inference and Tree Uncertainty in Comparative Analysis. Extended results are reported in the *SI Appendix*. Using exon capture approaches (26, 27), we assembled two main phylogenomic data matrices: 1) an expanded supermatrix that includes all genes and taxa sequenced for this study, with the

addition of GenBank sequences aimed at increasing taxonomic coverage for downstream comparative analyses (1,115 exons and 474,132 nucleotide sites for 110 out of ca. 136 species; 37% missing cells), and 2) a reduced (phylogenomic-only) matrix obtained with a matrix reduction algorithm, used to assess the sensitivity of phylogenomic results to missing data (1,047 exons and 448,410 nucleotide sites for 84 species; 16% missing cells). We conducted phylogenomic analyses using maximum likelihood (ML) and coalescent-based approaches. Inferred trees were resolved with strong support and are largely congruent among tested approaches and with results from previous studies (22, 26, 28–31). All analyses invariably resolved seven major clades (Fig. 1 and *SI Appendix*, Figs. S2–S5), confirming that the family Lutjanidae, as defined by many studies (e.g., refs. 23 and 32), is nonmonophyletic with fusiliers (Caesionidae) deeply nested within the broader snapper clade (33). The relationships estimated with the expanded matrix were highly consistent with those based on the reduced matrix, providing a robust phylogenomic framework for downstream comparative analyses.

In addition to expanded and reduced datasets, we also analyzed 13 (largely nonoverlapping) gene subsets derived from the expanded matrix, each with a sufficient number of genes to overcome sampling error (*Dataset S4*). The resulting trees reflect uncertainty in divergence times and phylogenetic relationships, an approach that is fundamentally different from the common practice of conducting comparative analyses using “pseudoreplicated” trees obtained from a Bayesian posterior distribution estimated with a single dataset, typically consisting of a handful of genes. We estimated a total of 28 trees that include all taxa using both concatenation-based ML (RAxML) and coalescent-based (ASTRAL-II) approaches applied to the expanded matrix and its 13 subsets. The divergence-time estimates, using the 28 input topologies and 7 calibration points (*SI Appendix*, Table S5), generally agreed with those from previous multilocus studies for the family (26, 28–31, 34; *SI Appendix*, Figs. S12–S14 and Table S5 and *Dataset S5*). Our divergence-time estimations date the age of crown lutjanids to the middle Eocene (~46 Ma, 95% highest posterior density [HPD]: 40 to 49 Ma) and the stem age close to the K–Pg boundary (~64.2 Ma, 95% HPD: 57.6 to 68.6 Ma).

The Geography of Habitat Transitions. To assess the geographic prevalence of evolutionary transitions in Lutjanidae, we performed ancestral habitat and ancestral range estimations. To infer the history of habitat transitions, we first assigned species into two major habitat categories (benthic and midwater dwellers) and accounted for uncertainty in habitat coding for 13 species using three different probability schemes (see *Materials and Methods* and *SI Appendix*). Because the implementation of different schemes had an effect on the SIMMAP reconstructions (Fig. 1 and *SI Appendix*, Figs. S8–S11), the most likely tip states inferred with each scheme (averaged over the 28 trees in each case) were used for all other downstream analyses that required a priori habitat categorization of tips (e.g., trait evolution and convergence and state-dependent diversification). The results of these alternative analyses are reported in combination in the main text and individually in the *SI Appendix*.

To estimate ancestral ranges, we built a presence–absence matrix of species distribution using alternative biogeographic schemes (35, 36; *Dataset S3*). Inferences of ancestral ranges using BioGeoBEARS (37) indicate an Indo-West Pacific Ocean origin for lutjanids, with subsequent independent colonization events of the Atlantic (six times) and the eastern Pacific (nine times) via multiple routes (Fig. 1 and *SI Appendix*, Figs. S12–S14 and see *SI Appendix*, *Supplementary Results* for an expanded account on the biogeography). By merging results of ancestral habitat and ancestral range inferences, we find support for benthic habitats as the most likely ancestral condition, with

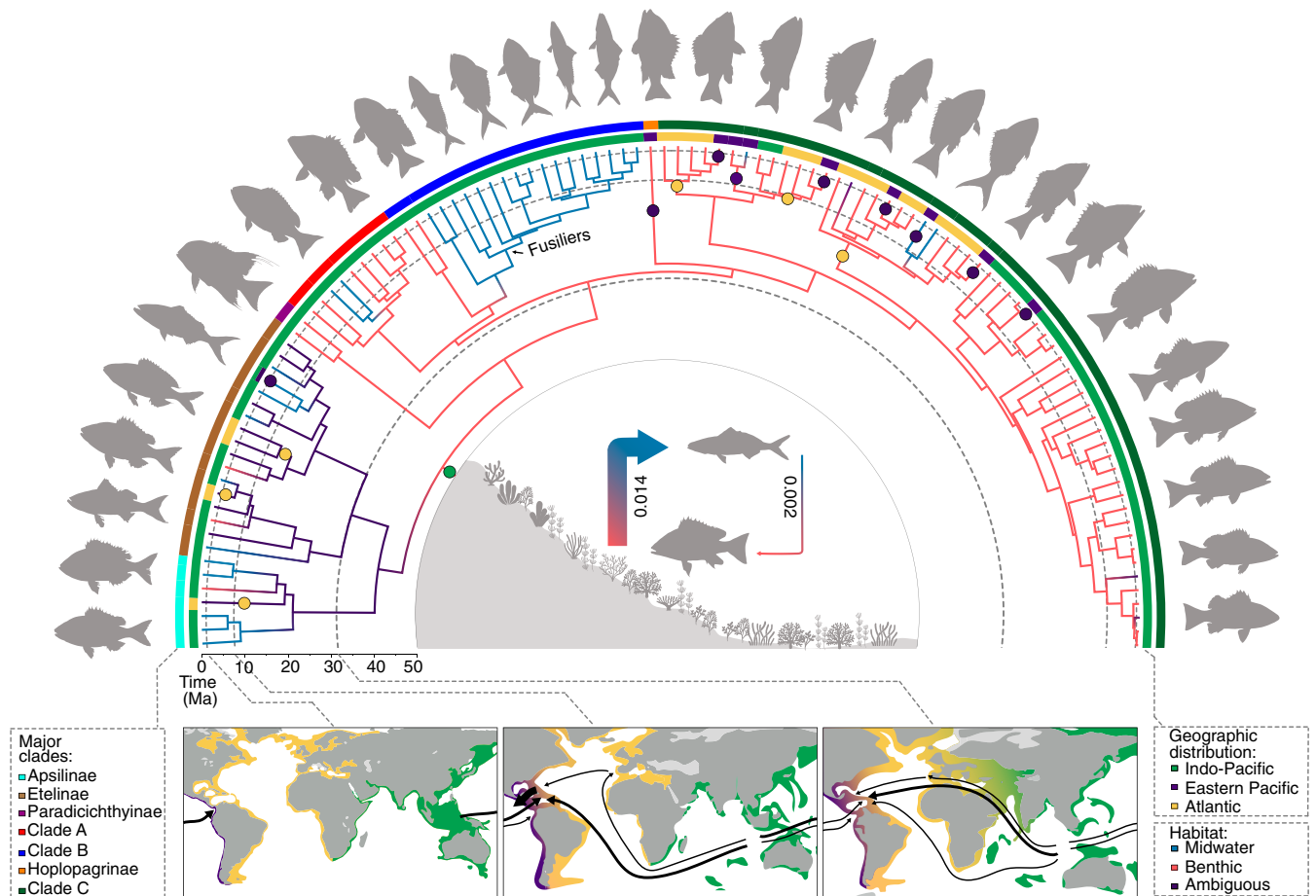


Fig. 1. Phylogeny, habitat transitions, and biogeography of snappers and fusiliers. The tree shown is derived from a concatenation-based maximum-likelihood analysis of 1,115 exons, with node ages estimated from a time-calibrated analysis using seven calibration points in MCMCTree. The habitat reconstructions for benthic and midwater lineages, shown as colored branches in the tree, account for phylogenetic uncertainty (28 trees) and habitat coding ambiguity (13 tips with uncertain or multistate habitats; see [Dataset S2](#)). The color gradients along branches denote habitat transitions; the purple branches indicate lineages with ambiguous habitats based on reconstructions using alternative coding schemes ([SI Appendix, Figs. S8–S11](#)). The colored circles indicate colonization events (inferred with BioGeoBEARS; see also [SI Appendix, Figs. S8 and S12–S14](#)) of the Atlantic (yellow circles) and the tropical eastern Pacific (purple circles) from Indo-Pacific lineages (center of origin; green circle). The arrows in the maps depict reconstructed colonization routes by different lineages in three time slices: 50 to 12 Ma (mean, 31 Ma), before the closure of Tethys Seaway; 12 to 2.8 Ma (mean, 7.4 Ma), after closure of Tethys Seaway and before the closure of the Isthmus of Panama; and 2.8 Ma to present (mean, 1.4 Ma), after the closure of the Isthmus of Panama. The thickness of the arrows is proportional to the number of lineages that colonized via each route; for some lineages, colonization routes are uncertain, and thus all alternative routes are depicted. The arrows in the central panel show the transition rates between benthic and pelagic habitats, as estimated with HiSSE (see also [SI Appendix, Tables S10–S12](#)).

independent and recurrent invasions of the water column by benthic lineages at least once within each of the three major oceanic basins (Fig. 1 and [SI Appendix, Figs. S8–S11](#)). While the Indo-Pacific features more transitions than other basins, our inferences highlight the deterministic nature and ubiquity of the transitions (Fig. 1 and [SI Appendix, Fig. S8](#)).

Ecomorphological Convergence. To test whether invasions of the water column are associated with a set of convergent high-fitness solutions (e.g., refs. 38 and 39), we assembled a specimen imagery database and built three alternative datasets based on digitized landmarks: 1) a full-body shape dataset, 2) a body-only dataset, and 3) a fins-only dataset ([SI Appendix, Fig. S1 and Table S7](#)). Traitgram-informed morphospaces (Fig. 2) show that different lutjanid midwater lineages independently evolved slender bodies and furcate caudal fins, an indication of strong ecologically driven morphological convergence. This pattern is further confirmed based on the threshold model (40), where the full-body shape dataset reveals a substantial correlation between the two habitat states and principal component 1 (PC1) ($r^2 =$

0.57 to 0.67), which captured differences in body elongation and caudal fin shape. The remaining three PC axes (PC2 to PC4) summarize further relevant aspects in fin-shape variation and ornamentation. We detected the same pattern for the body-only ($r^2 = 0.42$ to 0.57) and fins-only ($r^2 = 0.56$ to 0.69) datasets, where only PC1 exhibits significant correlations. We found an extensive overlap between benthic and midwater species at the lower PC axes, reflecting lower correlations between the PC2 and PC4 and habitat occupancy data ($r^2 = 0.07$ to 0.24 for the full-body shape dataset). These results suggest that ecomorphological convergence is less clearly associated with PC2 to PC4 axes than it is with the main PC1 axis ([SI Appendix, Fig. S15](#)).

We used a series of complementary approaches to further assess the scope and strength of convergence. We first compared the relative fit of a set of models of trait evolution in a multivariate framework [mvMORPH (41)], the results of which show split support for the two multiselective regime models (multiselective regime BM [BMM] and multiselective regime Ornstein-Uhlenbeck [OUM]; see [Materials and Methods](#)), with distinct selective regimes corresponding to the two different habitat

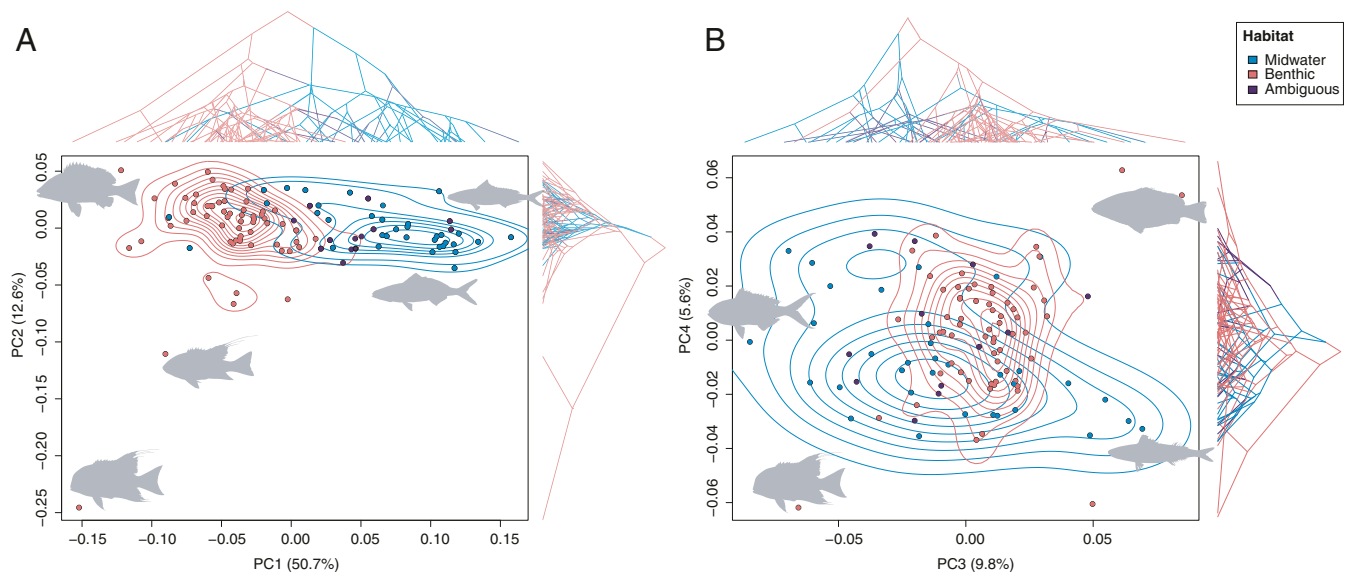


Fig. 2. The traitgram-informed morphospaces for lutjanids illustrating ecomorphological partitioning and convergence across benthic and midwater lineages, as estimated using the full-body dataset. The contour lines represent the two-dimensional density distributions of the species in each habitat state. The traitgrams overlain along PC axes depict the phylogeny in Fig. 1, including the ancestral habitat reconstructions estimated with SIMMAP (A, PC1 versus PC2; B, PC3 versus PC4). The color gradients along branches denote habitat transitions; the purple branches and data points indicate lineages with ambiguous habitats based on alternative coding schemes. The branches shifting from red to blue along PC1 extremes highlight convergent evolution in midwater lineages. The parenthetical values indicate the total variance explained by each PC axis.

categories (Fig. 3 *A* and *B* and *SI Appendix*, Figs. S16–S18). We then estimated the difference in trait distance between tips in the trees and the maximum distance between those taxa through their evolutionary history [*conevol*, C1 to C4 metrics (42)] and quantified phenotypic similarity based on phylogenetic relatedness [Wheatsheaf index or w (43)]. The C1 to C4 statistics were all significant for the three alternative morphometric datasets, with midwater lineages shortening about half of their phenotypic distance by subsequent convergent evolution (C1 = 37 to 45%; *SI Appendix*, Table S8). Likewise, results using the Wheatsheaf index ($w = 1.3$ to 1.4 ; *SI Appendix*, Figs. S19 and S20) identified significantly stronger convergence in midwater species than would be expected from a random distribution of trait values simulated under a Brownian Motion (BM) model ($P < 0.01$). All w values were similar, and the CI overlapped among the three alternative morphometric datasets, suggesting that both body shape and fin morphologies have similar strength in convergent evolution. To further validate these results, we calculated w using benthic species as focal clades. In this case, w was significantly smaller than the values simulated under BM in all three morphometric datasets ($w = 0.83$ to 0.88 ; $P > 0.95$), suggesting that morphological diversity is high among benthic dwellers, whereas strong convergent evolution is mostly restricted to midwater lutjanids. Finally, we assessed the optimal number of selective regimes under an Ornstein-Uhlenbeck process without a priori designation of habitats [ℓ 1ou and SURFACE (44, 45)]. The ℓ 1ou (multivariate) and SURFACE (univariate) analyses also identified multiple instances of convergence across lineages with adaptive peaks between clades with similar body plans (deep or slender bodies). For most datasets, the number of nonconvergent (adaptive) peak shifts was higher than the number of convergent peaks (*SI Appendix*, Table S9 and Dataset S6), and ℓ 1ou simulations revealed a significantly greater number of convergent shifts than would be expected by chance (*SI Appendix*, Figs. S21–S23). SURFACE analyses identified a greater number of convergent regimes (*SI Appendix*, Fig. S24) than ℓ 1ou

for most datasets. Taken together, our results suggest the overall convergence of many lineages to multiple, shared adaptive peaks in body shape ecomorphology (*SI Appendix*, Fig. S25).

Transition Rates and Diversification in Benthic and Midwater Lineages. We gauged the preference for different habitat states and their effect on rates of habitat transitions (Fig. 3*F*) and lineage diversification (Fig. 3*E*), providing a test for the prediction that the adoption of the midwater lifestyle may result in an evolutionary ratchet. For 20 out of the 28 trees, model-fitting comparisons supported a state-dependent model (Fig. 3 *C* and *D*) that incorporates a hidden state (*SI Appendix*, Tables S2–S4) associated with benthic lineages (hidden state speciation and extinction [HiSSE] benthic; *SI Appendix*, Fig. S27*A*). While the “HiSSE benthic” model is not decisively favored across all trees, finding in some cases substantial support for two alternative null models, under this model, net diversification rates (speciation minus extinction) are roughly two-times faster in benthic lineages than their midwater counterparts. The results obtained with HiSSE were consistent with those using the nonparametric FiSSE (fast, intuitive state-dependent speciation–extinction) and parametric BiSSE (binary state speciation and extinction) approaches (*SI Appendix*, Fig. S29 and Tables S10–S12), identifying support for habitat-dependent diversification. In agreement with our hypotheses, benthic dwellers tend to show faster rates of net diversification than midwater species, including both faster speciation and slower extinction (*SI Appendix*, Tables S10–S12). The HiSSE analyses using a model that accounts for habitat-dependent diversification (HiSSE benthic) identified asymmetric transition rates, favoring the expectations that benthic-to-midwater transitions (mean $q = 0.014$) are more frequent than midwater-to-benthic transitions (mean $q = 0.002$; Figs. 1 and 3*F* and *SI Appendix*, Fig. S27*B*).

Discussion

By implementing integrative comparative analyses in a robust phylogenomic framework, we find strong evolutionary determinism in benthic-to-midwater transitions along the water column in snappers

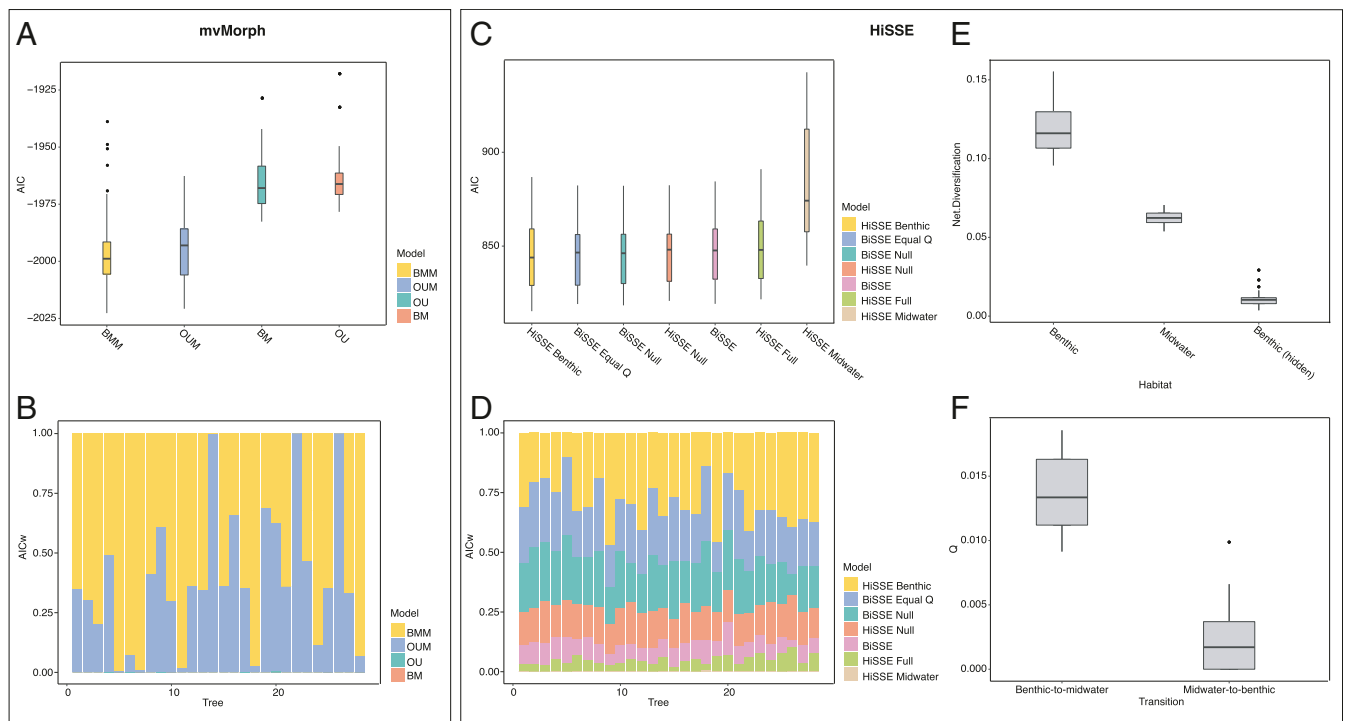


Fig. 3. The model-fitting comparisons and lineage diversification parameters estimated by accounting for phylogenetic uncertainty (28 trees) and habitat coding ambiguity (13 tips with uncertain or multistate habitats). The comparisons of alternative models of morphological evolution using the full-body dataset: (A) distribution of the Akaike information criterion (AIC) values for the four alternative models of continuous trait evolution (BM, OU, BMM, and OUM) and (B) AIC weights (AICw) of each alternative model and tree. The comparisons for alternative models of lineage diversification: (C) distribution of AIC values for seven alternative SSE models (*SI Appendix, Tables S2–S4*) and (D) AICw for each SSE model based on each of the 28 trees. The estimated lineage diversification parameters: (E) net-diversification values for the three habitat states and (F) transition rates (Q) between benthic and midwater states.

and fusiliers. While deep-body plans in benthic lineages enhance maneuverability in complex habitats with crevices, such as coral reefs or rocky bottoms, primarily benthic lineages that independently transitioned into midwater habitats consistently evolved elongate, fusiform bodies and furcate caudal fins, convergent adaptations that reduce hydrodynamic drag and recognizably promote increased swimming performance (7, 13, 22, 38, 39, 46–48)—a strong match between form and function (49). This deterministic process is ubiquitous at both temporal and spatial scales, with transitions taking place in lutjanid lineages of different ages and within all major marine biogeographic regions. Within each of the three major oceanic realms, benthic lutjanid lineages invaded the water column at least once. Furthermore, while the oldest benthic-to-midwater transition we identified was at ca. 40 Ma (Apsilinae + Eteolinae clade), more recent divergences (e.g., ~5 Ma) include sister species that lie at extremes of this ecological axis (e.g., *Lutjanus colorado* and *L. aratus*). Snappers and fusiliers thus bridge the gap of this recurrent ecological divergence that is well documented at shallower ends of the evolutionary continuum in model clades such as sticklebacks, cichlids, and whitefish (11, 14–19) and more ancient animal lineages such as sharks and aquatic tetrapods (8).

The independent evolution of similar phenotypic traits in response to the adoption of similar habitat regimes is a well-characterized indicator of evolutionary convergence. Recurrent transitions are thus indicative of strong evolutionary determinism as a result of similar use of the niche space along the benthic–pelagic axis. The convergent morphologies among midwater species strongly suggest that lineages with independent evolutionary histories but similar habitat preferences are drawn toward similar adaptive optima. Unlike patterns observed among midwater lutjanids, benthic lineages reveal higher phenotypic

diversity and weaker convergence. These differences may be the result of greater levels of niche diversity in benthic habitats (50). Similar outcomes are observed at shallower evolutionary scales in European whitefishes (19) and cichlids in Lakes Apoyo and Xiloá in Nicaragua (18), where independent radiations each harbor a single elongated limnetic phenotype and a flock of more variable benthic lineages.

While the focus of this study is on convergent evolution, it is worth emphasizing the strength of evolutionary forces driving phenotypic divergence in body plans along the benthic–pelagic axis (9, 12, 13, 50, 51). Midwater lineages with slender bodies are typically a subclade of more generalized deep-bodied benthic groups, and this ecological partition in phylogenetically nested clades has often led to taxonomic misclassifications. This explains why the midwater and planktivorous fusiliers are often placed in their own family, Caesionidae (refs. 52–58; <http://www.fishbase.org>). In his revision of lutjanid relationships, Johnson (23) noted that fusiliers feature unique traits among midwater lutjanids, including “an innovative restructuring of the functional complex of the upper jaw (permitting extreme protrusibility for planktivorous feeding) and an alteration of the basic body configuration (providing greater and more rapid swimming ability).” Remarkably, some adaptive landscape analyses that detected a single adaptive shift in Lutjanidae (*SI Appendix, Figs. S14–S17*) identified the shift at the base of the fusilier clade—a direct quantification of the distinct morphology in this group. Similar instances are increasingly being documented in many other marine fishes. A prime example includes the midwater Boga in the Caribbean, formerly listed as *Inermia vittata* in the family Emmelichthyidae but recently shown to be a derived grunt [Haemulidae (59)]. A more extreme case comprises the picarels, previously placed in Centracanthidae, a family that is polyphyletically

nested within benthic porgies in the family Sparidae (60). Benthic porgy lineages have thus independently colonized the water column multiple times, leading to strong, if not perfect, instances of convergent “centrarchid” body plans. These divergences can even cross species boundaries, as demonstrated by the benthic Coney (*Cephalopholis fulva*), which is known to practice “intergeneric hybridization” with the midwater Creole-fish [formerly *Paranthias colonus*, now *C. colonus* (61)]. In all these cases, it is recurrently the planktivorous and slender midwater subclade or species that is derived from the more generalized benthic clade, a result of speciation and adaptation by shifting dietary resources along the water column axis (62–64), ultimately creating taxonomic confusion.

The midwater lifestyle may be an evolutionary ratchet due to overall lower levels of diversity in these habitats, both taxonomically and morphologically, compared to the more species-rich benthic communities. For instance, relatively ancient species-poor clades of marine fishes, such as billfishes, swordfishes, and marlins, suggest slow diversification in pelagic environments (12). This is, however, not necessarily the case for other pelagic fish clades (e.g., Scombriformes, Clupeiformes) or midwater lutjanid lineages. While most tests identified higher diversification rates in benthic lineages (Fig. 1 and *SI Appendix, Figs. S27–S29*), which are roughly twice as fast compared to the midwater counterparts (Fig. 3 *E* and *F*), HiSSE analyses failed to support a model of habitat-dependent diversification in ~30% of the trees. A remarkable exception includes the fusiliers, a relatively young lutjanid subclade (~16 Ma) that comprises 23 species. Fusilier species may school together with congeners and other pelagic species. For instance, the mottled fusilier (*Dipterygnotus balteatus*), the only lutjanid that has adopted an exclusive pelagic lifestyle as an adult, is often caught together with clupeoids (herrings and anchovies). These observations suggest that midwater lutjanid species present important functional differences and elevated levels of niche partitioning, which may explain the occurrence of species-rich pelagic clades. Ultimately, however, niche partitioning in the resource-poor and homogeneous pelagic environment may result in population density declines and increased trophic specializations, mechanisms that are known to increase extinction vulnerability over long time-scales (65). State-dependent diversification analyses provide some support for these ideas, identifying remarkably faster rates of extinction in midwater than benthic lineages (*SI Appendix, Tables S10–S12*).

Snappers and fusiliers exhibit strong but imperfect morphological convergence (66) associated with habitat transitions. Whereas functional traits associated with ecological partitioning along the benthic–pelagic axis have consistently resulted in similar evolutionary outcomes, some lineages have evolved distinct nonconvergent phenotypic adaptations. Exceptions include deep-bodied lineages that tend to occur higher in the water column, such as species in the genus *Macolor*. As pointed out by Hobson (67), “Obviously many conflicting pressures have differentially affected the morphologies of the various fishes that forage on tiny organisms in the midwaters.” Thus, although the slender body plan is pervasive among midwater dwellers, a limited set of alternative phenotypic solutions can meet the conditions necessary to thrive in pelagic habitats [i.e., many-to-one mapping (68)]. Outside Lutjanidae, remarkable departures from typical streamlined body shapes found in most oceanic pelagic vertebrates include the slow-swimming ocean sunfishes, butterflyfishes, moonfish, opah, and tripletails, which feature deep and laterally compressed body plans. Although we did not examine diets and feeding morphology in this study, a key factor that triggers the invasion of the water column is the trophic adaptation to planktivory. Morphological convergence has been reported in many groups that share specialized dietary shifts to planktivory (e.g., butterflyfishes, wrasses, angelfishes, damselfishes, and sea

basses; 46, 63, 69, 70). The ecological opportunity for the exploitation of different resources has thus repeatedly promoted morphological and behavioral adaptations associated with water-column transitions (63, 71).

In conclusion, we find strong evidence of evolutionary convergence in major traits related to body elongation and fin morphology as a result of ecological transitions into pelagic habitats, ultimately reinforcing the deterministic role of evolution driven by similar ecological pressures. Our research shows incursions into the water column that are strongly linked to patterns of evolutionary convergence in body plans. We also have identified asymmetric habitat transitions and slower rates of lineage diversification associated with incursions into midwater habitats. The fact that these independent transitions took place in all major biogeographic regions further reinforces the deterministic nature of evolution. While convergent evolution associated with the adoption of the pelagic lifestyle has governed the mode of diversification in Lutjanidae, future work should consider whether this conclusion can be generalized to support other habitat transitions along the benthic–pelagic axis as a primary mechanism of diversification in fishes.

Materials and Methods

Taxonomic Sampling and Genomic Data. Extended materials and methods are reported in the *SI Appendix, Supplementary Materials and Methods*. Our genomic sampling includes 85 newly sequenced species of snappers and fusiliers from specimens deposited in multiple fish collections. To further expand the taxonomic scope, we retrieved sequences for 25 additional in-group species from GenBank. Our combined dataset contains 110 species plus 14 out-groups (*Dataset S1*). High-quality DNA extractions were sent to Arbor Biosciences for target enrichment and sequencing. Our target capture probes are based on a set of 1,104 single-copy exons optimized for ray-finned fish phylogenetics (26, 27). We also included 15 legacy exons into the probe set. After performing standard procedures for sequence quality control and assembly, we aligned exons by taking into account their reading frames.

Accounting for Missing Data in Phylogenomic Inference. We assembled two main data matrices: 1) an expanded matrix with all genes and taxa, including GenBank sequences, and 2) a reduced matrix obtained with the MARE (matrix reduction) package (72). For each matrix, we determined the best-fitting partitioning schemes and nucleotide substitution models for both genes and codon positions using PartitionFinder2 (73). We also assembled 13 additional subsets by manually subsampling the expanded matrix (see details below). For all datasets, we estimated ML trees in RAxML version 8.2.4 (74) using the partition output obtained with PartitionFinder2. The species trees were then inferred with ASTRAL-II version 4.7.12 (75) using individual RAxML-based gene trees as input.

Accounting for Topological and Temporal Uncertainty. We built a number of largely independent subsets (subsampling from the expanded matrix), each with a sufficient number of genes to overcome sampling error by capturing our knowledge of the phylogeny of the group in the best possible manner. We assembled 13 subsets (seven with 89 loci and six with 90 loci), all of which overlap in only four genes, thereby maintaining the same set of species. As input topologies for phylogenetic dating in MCMCTree (see below), we inferred a total of 28 phylogenetic trees using both RAxML and ASTRAL-II. Two trees were estimated using the complete expanded matrix, including a “master tree” based on the RAxML topology; the remaining 26 trees were obtained with the 13 subsets subsampled from this matrix. While most downstream comparative analyses used the 28 trees, some were computationally demanding and therefore were based on the “master tree” only (indicated whenever applicable).

Phylogenetic Dating. We conducted divergence time estimations using the MCMCTree package as implemented in the program PAML version 4.9a (76), which can handle genome-scale datasets in a Bayesian framework (77). Because MCMCTree running time depends more on the number of partitions defined rather than the number of genes included (77), all 28 subsets used only two partitions (first + second and third codon positions). We applied seven calibration points, two based on fossils with uniform distributions and

five based on a geological event with flat-tailed Cauchy distributions (*SI Appendix, Table S1*).

Inferences of Ancestral Habitats and Ancestral Ranges. The habitat occupancy dataset (*Dataset S2*) was compiled by aggregating information from a wide range of sources, including FishBase, the primary literature, and by consulting experts. The reconstructions performed used a broad sampling of 97 haemulid out-groups (13). To account for 13 Lutjanid species with uncertain habitat occupancy, we implemented ancestral character reconstructions that take into account tip-state ambiguity based on stochastic character mapping [SIMMAP (78)], as implemented in the R package phytools (79). We coded these ambiguous tips using three alternative probability schemes: 0.1 benthic/0.9 midwater, 0.50 benthic/0.50 midwater, and 0.9 benthic/0.1 midwater (*SI Appendix*).

We also classified species according to their geographical ranges. We built a presence/absence matrix of species considering six recognized marine biogeographic regions (35, 36; *Dataset S3*): West Indian Ocean (WIO), Central Indo-Pacific (CIP), Central Pacific (CP), Tropical Eastern Pacific (TEP), Western Atlantic (WA), and Eastern Atlantic (EA). Ancestral range estimations were performed using the R package BioGeoBEARS (37). Using the “master tree” as the input phylogeny, 12 different biogeographic models were tested. We analyzed each model using three time slices according to different geological events (see *SI Appendix* for details on models and matrices used for BioGeoBEARS). For simplicity, we summarized ancestral ranges into three major ocean realms by merging EA and WA into the Atlantic; WIO, CIP, and CP into the Indo-Pacific; and leaving the TEP as originally coded (Fig. 1).

Geometric Morphometrics on Body Shape. The laterally compressed body plan of snappers and fusiliers makes this group well suited for the summarization of morphological diversity using two-dimensional geometric morphometric approaches. We assembled a specimen imagery dataset from museum collections or curated images retrieved from online repositories. To account for intraspecific variation, our dataset includes one to four individuals from each of the 110 species (total, 413 individuals; mean, 3.72 individuals per species; *Dataset S1*). We generated three alternative datasets (following ref. 80) based on digitized landmarks: 1) a full-body and fin shape dataset, 2) a body-only dataset, and 3) a fins-only dataset (*SI Appendix, Materials and Methods and Fig. S1*). For each dataset, we performed Procrustes superimposition, calculated species-average coordinates, and conducted both standard and phylogenetically corrected principal component analyses (81, 82). Finally, we determined the number of meaningful PC axes using the brokenstick model (83, 84), which minimizes the loss of signal while avoiding noise from less relevant axes.

Convergence Analyses. To assess the scale and nature of convergence among taxa exhibiting similar habitat regimes, we ran a set of recently proposed multivariate phylogenetic comparative methods for each of the three alternative morphological datasets (full body shape, body only, and fins only).

We first tested the relative fit of a range of evolutionary models using the package mvMORPH (41). These include a single-rate BM model, a single-regime OU model, and multiregime BMM and OUM models. We also tested for correlation between habitat occupation and the four most relevant PC axes using the threshold model, which assesses the association between a discrete trait and a continuous character that covary according to an underlying, unobserved trait called liability (85). We explicitly tested for convergent evolution using the C1 to C4 distance-based metrics implemented in *convevol* (ran using the “master tree”) as well as the Wheatsheaf index implemented in the R package Windex (43). Finally, we used other data-driven approaches, as implemented in the R package *rlou* version 1.42 (44) and SURFACE version 0.4 (45), to estimate the optimal number of selective regimes under an OU process applied to the least absolute shrinkage and selection operator.

State-Dependent Diversification. We evaluated the influence of habitat type (benthic versus midwater dwellers) on lineage diversification dynamics using state-dependent speciation and extinction (SSE) approaches (86). We applied HiSSE, an SSE approach that tests the relative fit of a set of alternative branching models while accounting for hidden states. For comparison, and to estimate habitat-dependent evolutionary rates in a Bayesian framework, we also used BiSSE as implemented in the R package diversitree (87). Finally, we used the nonparametric FiSSE approach, which has shown to be robust to phylogenetic pseudoreplication and model misspecification (88). See *SI Appendix* for details.

Data Availability. Raw sequencing reads are available at National Center for Biotechnology Information Sequence Read Archive BioProject (number PRJNA630817). Alignments, trees, and code data have been deposited in Figshare (DOI: 10.6084/m9.figshare.13000100). All other study data are included in the article and supporting information.

ACKNOWLEDGMENTS. We are thankful for the extensive and insightful comments by D. Johnson and two anonymous reviewers that helped improve the quality of our study. We thank O. Domínguez, Universidad Michoacana de San Nicolás de Hidalgo, for providing samples. M. Stimson and M. Bagger (The George Washington University) conducted DNA extractions. E. Santaquiteria provided artistic illustrations. Bioinformatic analyses were facilitated by the High-Performance Computing Facility of the University of Puerto Rico–Rio Piedras (funded by IDeA Networks of Biomedical Research Excellence [INBRE] Grant P20GM103475) and the University of Oklahoma Supercomputing Center for Education & Research. This research was supported by NSF grants DEB-1932759 and DEB-1929248 to R.B.-R., DEB-1457426 and DEB-1541554 to G.O., DEB-1541552 to C.C.B., and DEB-2015404 to D.A. M.R.-S. was supported by a postdoctoral fellowship from Colciencias (Grant 848-2019). Financial support was provided from the Office of the Vice President for Research and Partnerships and the Office of the Provost, University of Oklahoma.

1. S. J. Gould, *Wonderful Life: The Burgess Shale and the Nature of History* (W. W. Norton & Company, 1989).
2. J. B. Losos, Contingency and determinism in replicated adaptive radiations of island lizards. *Science* **279**, 2115–2118 (1998).
3. A. A. Agrawal, Toward a predictive framework for convergent evolution: Integrating natural history, genetic mechanisms, and consequences for the diversity of life. *Am. Nat.* **190**, S1–S12 (2017).
4. J. B. Losos, Convergence, adaptation, and constraint. *Evolution* **65**, 1827–1840 (2011).
5. D. B. Wake, M. H. Wake, C. D. Specht, Homoplasy: From detecting pattern to determining process and mechanism of evolution. *Science* **331**, 1032–1035 (2011).
6. Z. D. Blount, R. E. Lenski, J. B. Losos, Contingency and determinism in evolution: Replaying life's tape. *Science* **362**, eaam5979 (2018).
7. M. D. Burns, B. L. Sidlauskas, Ancient and contingent body shape diversification in a hyperdiverse continental fish radiation. *Evolution* **73**, 569–587 (2019).
8. G. R. McGhee, *Convergent Evolution: Limited Forms Most Beautiful* (The MIT Press, 2011).
9. E. D. Buresh, J. M. Holcomb, M. Tan, J. W. Armbruster, Ecological diversification associated with the benthic-to-pelagic transition by North American minnows. *J. Evol. Biol.* **30**, 549–560 (2017).
10. T. Claverie, P. C. Wainwright, A morphospace for reef fishes: Elongation is the dominant axis of body shape evolution. *PLoS One* **9**, e112732 (2014).
11. C. D. Hulse, R. J. Roberts, Y. H. E. Loh, M. F. Rupp, J. T. Streelman, Lake Malawi cichlid evolution along a benthic/limnetic axis. *Ecol. Evol.* **3**, 2262–2272 (2013).
12. E. Ribeiro, A. M. Davis, R. A. Rivero-Vega, G. Ortí, R. Betancur-R, Post-cretaceous bursts of evolution along the benthic-pelagic axis in marine fishes. *Proc. Biol. Sci.* **285**, 20182010 (2018).
13. J. Tavera, A. Acero P, P. C. Wainwright, Multilocus phylogeny, divergence times, and a major role for the benthic-to-pelagic axis in the diversification of grunts (Haemulidae). *Mol. Phylogenet. Evol.* **121**, 212–223 (2018).
14. J. A. Walker, Ecological morphology of lacustrine threespine stickleback *Gasterosteus aculeatus* L. (Gasterosteidae) body shape. *Biol. J. Linn. Soc. Lond.* **61**, 3–50 (1997).
15. H. D. Rundle, L. Nagel, J. W. Boughman, D. Schluter, Natural selection and parallel speciation in sympatric sticklebacks. *Science* **287**, 306–308 (2000).
16. C. Clabaut, P. M. E. Bunje, W. Salzburger, A. Meyer, Geometric morphometric analyses provide evidence for the adaptive character of the Tanganyikan cichlid fish radiations. *Evolution* **61**, 560–578 (2007).
17. W. J. Cooper et al., Benthic-pelagic divergence of cichlid feeding architecture was prodigious and consistent during multiple adaptive radiations within African rift-lakes. *PLoS One* **5**, e9551 (2010).
18. K. R. Elmer et al., Parallel evolution of Nicaraguan crater lake cichlid fishes via non-parallel routes. *Nat. Commun.* **5**, 5168 (2014).
19. K. Præbel et al., Ecological speciation in postglacial European whitefish: Rapid adaptive radiations into the littoral, pelagic, and profundal lake habitats. *Ecol. Evol.* **3**, 4970–4986 (2013).
20. M. Friedman, Explosive morphological diversification of spiny-finned teleost fishes in the aftermath of the end-Cretaceous extinction. *Proc. Biol. Sci.* **277**, 1675–1683 (2010).
21. W. P. Davis, R. S. Birdsong, Coral reef fishes which forage in the water column. *Helgol. Wiss. Meeresunters.* **24**, 292–306 (1973).
22. B. Frédérix, F. Santini, Macroevolutionary analysis of the tempo of diversification in snappers and fusiliers (Percomorpha: Lutjanidae). *Belg. J. Zool.* **147**, 17–35 (2017).
23. D. Johnson, *The Limits and Relationships of the Lutjanidae and Associated Families* (University of California Press, Berkeley, 1980).
24. J. S. Gray, Marine biodiversity: Patterns, threats and conservation needs. *Biodivers. Conserv.* **6**, 153–175 (1997).
25. M. A. Balisi, B. Van Valkenburgh, Iterative evolution of large-bodied hypercarnivory in canids benefits species but not clades. *Commun. Biol.* **3**, 461 (2020).

26. L. C. Hughes *et al.*, Comprehensive phylogeny of ray-finned fishes (Actinopterygii) based on transcriptomic and genomic data. *Proc. Natl. Acad. Sci. U.S.A.* **115**, 6249–6254 (2018).
27. L. C. Hughes *et al.*, Exon probe sets and bioinformatics pipelines for all levels of fish phylogenomics. *Mol. Ecol. Resour.*, 10.1101/2020.02.18.949735 (2020).
28. R. Betancur-R *et al.*, The tree of life and a new classification of bony fishes. *PLoS Curr.*, 10.1371/currrents.tol.53ba26640df0ccae755b165c8c26288 (2013).
29. R. Betancur-R *et al.*, Phylogenetic classification of bony fishes. *BMC Evol. Biol.* **17**, 162 (2017).
30. D. L. Rabosky *et al.*, An inverse latitudinal gradient in speciation rate for marine fishes. *Nature* **559**, 392–395 (2018).
31. T. J. Near *et al.*, Phylogeny and tempo of diversification in the superradiation of spiny-rayed fishes. *Proc. Natl. Acad. Sci. U.S.A.* **110**, 12738–12743 (2013).
32. J. Nelson, T. Grande, M. Wilson, *Fishes of the World* (John Wiley & Sons, Hoboken, NJ, 2016).
33. D. Johnson, Percomorph phylogeny—Progress and Problems. *Bull. Mar. Sci.* **52**, 3–28 (1993).
34. M. E. Alfaro, Resolving the ray-finned fish tree of life. *Proc. Natl. Acad. Sci. U.S.A.* **115**, 6107–6109 (2018).
35. M. Kulbicki *et al.*, Global biogeography of reef fishes: A hierarchical quantitative delineation of regions. *PLoS One* **8**, e81847 (2013).
36. M. D. Spalding *et al.*, Marine ecoregions of the world: A bioregionalization of coastal and shelf areas. *Bioscience* **57**, 573–583 (2007).
37. N. J. Matzke, BioGeoBEARS: BioGeography with Bayesian (and Likelihood) Evolutionary Analysis in R Scripts (Version 0.2, R Package, University of California, Berkeley, Berkeley, CA, 2013).
38. K. L. Feilich, G. V. Lauder, Passive mechanical models of fish caudal fins: Effects of shape and stiffness on self-propulsion. *Bioinspir. Biomim.* **10**, 036002 (2015).
39. P. W. Webb, Body form, locomotion and foraging in aquatic vertebrates. *Am. Zool.* **24**, 107–120 (1984).
40. J. Felsenstein, Using the quantitative genetic threshold model for inferences between and within species. *Philos. Trans. R. Soc. Lond. B Biol. Sci.* **360**, 1427–1434 (2005).
41. J. Clavel, G. Escarguel, G. Merceron, mvMORPH: An R package for fitting multivariate evolutionary models to morphometric data. *Methods Ecol. Evol.* **6**, 1311–1319 (2015).
42. C. T. Stayton, The definition, recognition, and interpretation of convergent evolution, and two new measures for quantifying and assessing the significance of convergence. *Evolution* **69**, 2140–2153 (2015).
43. K. Arbuckle, C. M. Bennett, M. P. Speed, A simple measure of the strength of convergent evolution. *Methods Ecol. Evol.* **5**, 685–693 (2014).
44. M. Khabbazian, R. Kriebel, K. Rohe, C. Ané, Fast and accurate detection of evolutionary shifts in Ornstein–Uhlenbeck models. *Methods Ecol. Evol.* **7**, 811–824 (2016).
45. T. Ingram, D. L. Mahler, SURFACE: Detecting convergent evolution from comparative data by fitting Ornstein–Uhlenbeck models with stepwise Akaike Information Criterion. *Methods Ecol. Evol.* **4**, 416–425 (2013).
46. S. T. Friedman, S. A. Price, A. S. Hoey, P. C. Wainwright, Ecomorphological convergence in planktivorous surgeonfishes. *J. Evol. Biol.* **29**, 965–978 (2016).
47. R. B. Langerhans, D. N. Reznick, “Ecology and evolution of swimming performance in fishes: Predicting evolution with biomechanics” in *Fish Locomotion: An Eco Ethological Perspective*, P. Domenici, B. G. Kapoor, Eds. (Science Publishers, Enfield, NH, 2010), pp. 200–248.
48. J. P. Velotta, S. D. McCormick, A. W. Jones, E. T. Schultz, Reduced swimming performance repeatedly evolves on loss of migration in landlocked populations of alewife. *Physiol. Biochem. Zool.* **91**, 814–825 (2018).
49. A. L. Pigot *et al.*, Macroevolutionary convergence connects morphological form to ecological function in birds. *Nat. Ecol. Evol.* **4**, 230–239 (2020).
50. S. T. Friedman *et al.*, Body shape diversification along the benthic-pelagic axis in marine fishes. *Proc. Biol. Sci.* **287**, 20201053 (2020).
51. S. A. Price *et al.*, Building a body shape morphospace of teleostean fishes. *Integr. Comp. Biol.* **59**, 716–730 (2019).
52. K. E. Carpenter, *Revision of the Indo-Pacific Fish Family Caesionidae (Lutjanioidea), with Descriptions of Five New Species* (Bishop Museum Press, 1987).
53. K. E. Carpenter, V. H. Niem, “Bony fishes part 3 (Menidae to Pomacentridae)” in *The Living Marine Resources of the Western Central Pacific* (FAO Species Identification Guide for Fishery Purposes, FAO, Rome, Italy, 2001), vol. 5, pp. 2791–3380.
54. K. E. Carpenter, Vol. 8. *Fusilier Fishes of the World: An Annotated and Illustrated Catalogue of Caesionid Species Known to Date* (FAO Species Catalogue, FAO, Rome, Italy, 1988).
55. K. E. Carpenter, A phylogenetic analysis of the Caesionidae (Perciformes: Lutjanioidea). *Copeia* **1990**, 692–717 (1990).
56. K. E. Carpenter, Optimal cladistic and quantitative evolutionary classifications as illustrated by fusilier fishes (Teleostei: Caesionidae). *Syst. Biol.* **42**, 142–154 (1993).
57. R. Fricke, W. N. Eschmeyer, R. van der Laan, Eschmeyer’s catalog of fishes: Genera, species, references. <http://researcharchive.calacademy.org/research/ichthyology/catalog/fishcatmain.asp>. Accessed 4 January 2019.
58. T. L. Miller, T. H. Cribb, Phylogenetic relationships of some common Indo-Pacific snappers (Perciformes: Lutjanidae) based on mitochondrial DNA sequences, with comments on the taxonomic position of the Caesioninae. *Mol. Phylogenet. Evol.* **44**, 450–460 (2007).
59. J. J. Tavera, A. Acero P, E. F. Balart, G. Bernardi, Molecular phylogeny of grunts (Teleostei, Haemulidae), with an emphasis on the ecology, evolution, and speciation history of new world species. *BMC Evol. Biol.* **12**, 57 (2012).
60. M. D. Sanciangco, K. E. Carpenter, R. Betancur-R, Phylogenetic placement of enigmatic percomorph families (Teleostei: Percomorphaceae). *Mol. Phylogenet. Evol.* **94**, 565–576 (2016).
61. M. T. Craig, P. A. Hastings, A molecular phylogeny of the groupers of the subfamily Epinephelinae (Serranidae) with a revised classification of the Epinephelini. *Ichthyol. Res.* **54**, 1–17 (2007).
62. D. R. Bellwood, L. van Herwerden, N. Konow, Evolution and biogeography of marine angelfishes (Pisces: Pomacanthidae). *Mol. Phylogenet. Evol.* **33**, 140–155 (2004).
63. S. R. Floeter, M. G. Bender, A. C. Siqueira, P. F. Cowman, Phylogenetic perspectives on reef fish functional traits. *Biol. Rev. Camb. Philos. Soc.* **93**, 131–151 (2018).
64. F. L. Lobato *et al.*, Diet and diversification in the evolution of coral reef fishes. *PLoS One* **9**, e102094 (2014).
65. B. Van Valkenburgh, X. Wang, J. Damuth, Cope’s rule, hypercarnivory, and extinction in North American canids. *Science* **306**, 101–104 (2004).
66. D. C. Collar, J. S. Reece, M. E. Alfaro, P. C. Wainwright, R. S. Mehta, Imperfect morphological convergence: Variable changes in cranial structures underlie transitions to durophagy in moray eels. *Am. Nat.* **183**, E168–E184 (2014).
67. E. S. Hobson, Feeding relationship of teleostean fishes on coral reefs in Kona, Hawaii. *Fish Bull.* **72**, 915–1031 (1974).
68. M. E. Alfaro, D. I. Bolnick, P. C. Wainwright, Evolutionary consequences of many-to-one mapping of jaw morphology to mechanics in labrid fishes. *Am. Nat.* **165**, E140–E154 (2005).
69. B. Frédéricich, L. Sorenson, F. Santini, G. J. Slater, M. E. Alfaro, Iterative ecological radiation and convergence during the evolutionary history of damselfishes (Pomacentridae). *Am. Nat.* **181**, 94–113 (2012).
70. P. F. Cowman, D. R. Bellwood, L. van Herwerden, Dating the evolutionary origins of wrasse lineages (Labridae) and the rise of trophic novelty on coral reefs. *Mol. Phylogenet. Evol.* **52**, 621–631 (2009).
71. W. J. Cooper, C. B. Carter, A. J. Conith, A. N. Rice, M. W. Westneat, The evolution of jaw protrusion mechanics is tightly coupled to benthic-pelagic divergence in damselfishes (Pomacentridae). *J. Exp. Biol.* **220**, 652–666 (2017).
72. B. Meyer, K. Meusemann, B. Misof, MARE: MATRIX REDUCTION—A tool to select optimized data subsets from supermatrices for phylogenetic inference (Version 0.1.2-rc, Zentrum fuer molekulare Biodiversitätsforschung [zmb] am ZFMK, Bonn, Germany, 2011).
73. R. Lanfear, P. B. Frandsen, A. M. Wright, T. Senfeld, B. Calcott, Partitionfinder 2: New methods for selecting partitioned models of evolution for molecular and morphological phylogenetic analyses. *Mol. Biol. Evol.* **34**, 772–773 (2017).
74. A. Stamatakis, RAxML version 8: A tool for phylogenetic analysis and post-analysis of large phylogenies. *Bioinformatics* **30**, 1312–1313 (2014).
75. S. Mirarab, T. Warnow, ASTRAL-II: Coalescent-based species tree estimation with many hundreds of taxa and thousands of genes. *Bioinformatics* **31**, i44–i52 (2015).
76. Z. Yang, PAML 4: Phylogenetic analysis by maximum likelihood. *Mol. Biol. Evol.* **24**, 1586–1591 (2007).
77. M. dos Reis, Z. Yang, “Bayesian molecular clock dating using genome-scale datasets” in *Evolutionary Genomics: Statistical and Computational Methods*, M. Anisimova, Ed. (Humana, New York, NY, 2019), vol. 1910.
78. J. P. Bollback, SIMMAP: Stochastic character mapping of discrete traits on phylogenies. *BMC Bioinformatics* **7**, 88 (2006).
79. L. J. Revell, phytools: An R package for phylogenetic comparative biology (and other things). *Methods Ecol. Evol.* **3**, 217–223 (2012).
80. A. B. George, M. W. Westneat, Functional morphology of endurance swimming performance and gait transition strategies in balistoid fishes. *J. Exp. Biol.* **222**, jeb194704 (2019).
81. D. C. Adams, E. Otárola-Castillo, Geomorph: An R package for the collection and analysis of geometric morphometric shape data. *Methods Ecol. Evol.* **4**, 393–399 (2013).
82. L. J. Revell, Size-correction and principal components for interspecific comparative studies. *Evolution* **63**, 3258–3268 (2009).
83. D. A. Jackson, No stopping rules in principal components analysis: A comparison of Heuristical and statistical approaches. *Ecol. Ecol. Soc. Am.* **74**, 2204–2214 (1993).
84. P. R. Peres-Neto, D. A. Jackson, K. M. Somers, How many principal components? Stopping rules for determining the number of non-trivial axes revisited. *Comput. Stat. Data Anal.* **49**, 974–997 (2005).
85. J. Felsenstein, A comparative method for both discrete and continuous characters using the threshold model. *Am. Nat.* **179**, 145–156 (2012).
86. W. P. Maddison, P. E. Midford, S. P. Otto, Estimating a binary character’s effect on speciation and extinction. *Syst. Biol.* **56**, 701–710 (2007).
87. R. G. Fitzjohn, Diversitree: Comparative phylogenetic analyses of diversification in R. *Methods Ecol. Evol.* **3**, 1084–1092 (2012).
88. D. L. Rabosky, E. E. Goldberg, FiSSE: A simple nonparametric test for the effects of a binary character on lineage diversification rates. *Evolution* **71**, 1432–1442 (2017).